

UNPUBLISHED PRELIMINARY DATA

05608-5-T

THE UNIVERSITY OF MICHIGAN

COLLEGE OF ENGINEERING
DEPARTMENT OF ENGINEERING MECHANICS
TIRE AND SUSPENSION SYSTEMS RESEARCH GROUP

Technical Report No. 2

The Rolling Tire Under Load

S. K. CLARK

N65-23669

(ACCESSION NUMBER)

38

(PAGES)

CR-62659

(NASA CR OR TMX OR AD NUMBER)

(THRU)

(CODE)

15

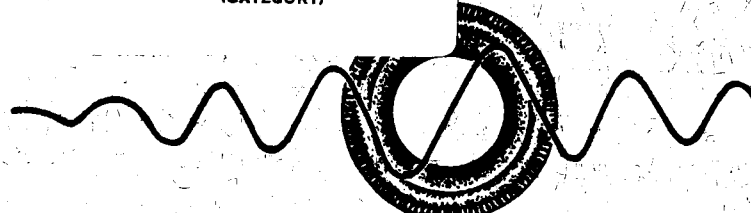
(CATEGORY)

GPO PRICE \$

OTS PRICE(S) \$

Hard copy (HC) \$2.00

Microfiche (MF) .50



Under contract with:

National Aeronautics and Space Administration

Grant No. NsG-344

Washington, D. C.

Administered through:

March 1965

OFFICE OF RESEARCH ADMINISTRATION • ANN ARBOR

THE UNIVERSITY OF MICHIGAN
COLLEGE OF ENGINEERING
Department of Engineering Mechanics
Tire and Suspension Systems Research Group

Technical Report No. 2

THE ROLLING TIRE UNDER LOAD

S. K. Clark

under contract with:

NATIONAL AERONAUTICS AND SPACE ADMINISTRATION
GRANT NO. NSG-344
WASHINGTON, D.C.

administered through:

OFFICE OF RESEARCH ADMINISTRATION ANN ARBOR

March 1965

The work described in this report was sponsored by
THE NATIONAL AERONAUTICS AND SPACE ADMINISTRATION
under Grant NsG-344. It has drawn heavily on previous work jointly sponsored by:

Firestone Tire and Rubber Company

General Tire and Rubber Company

B. F. Goodrich Tire Company

Goodyear Tire and Rubber Company

United States Rubber Company

TABLE OF CONTENTS

	Page
LIST OF FIGURES	vii
NOMENCLATURE	xi
I. ABSTRACT	1
II. INTRODUCTION	3
III. THE BASIC DYNAMIC MODEL FOR A ROLLING TIRE	5
IV. THE CONTACT PATCH REGION	15
V. CALCULATIONS AND EXAMPLES	19
VI. REFERENCES	31

LIST OF FIGURES

FIGURE	Page
1. Shell stress resultant conventions and nomenclature.	5
2. Narrow cylindrical shell notation.	7
3. Shell characteristics.	13
4. Geometry of intersection of elastic shell with rigid plane surface.	16
5. Contact patch length and position as a function of speed.	22
6. Vertical load as a functional of speed.	24
7. Drag force as a function of speed.	25
8. Maximum contact pressure as a function of speed.	27
9. Pressure distribution in contact patch for two different velocities.	28
10. Static load deflection curves—experimental vs. calculated.	30

NOMENCLATURE

English Letters

a	Undeformed radius of the cylindrical shell, a structural radius measured to the midline of the shell thickness
a_o	Undeformed geometric radius of the cylindrical shell, measured to the outside surface of the shell.
b_w	Width of cylindrical shell. This would normally correspond approximately to the tread width of a tire.
c	Viscous damping coefficient
c_1	Propagation velocity $\sqrt{E/p}$
\bar{c}	Dimensionless viscous damping coefficient
CWA	Dimensionless damping factor
\bar{D}	$E \cdot h$ (for a narrow shell or ring)
E	Young's modulus of shell material
h	Shell thickness
H	Shell deflection against a plane
k	Elastic stiffness of shell internal foundation
\bar{k}	Dimensionless elastic stiffness ka^2/Eh .
K	$Eh^3/12$ (for a narrow shell or ring)
KA	Dimensionless spring rate
N, M	Shell stress resultants
p	Pressure
p_o	Internal pressure
$p(\theta)$	External pressure

NOMENCLATURE (Concluded)

PA	Dimensionless internal pressure
PE	Dimensionless external pressure
PO	Dimensionless internal pressure
PQ	Dimensionless external pressure
Q	Shear force, lbs
t	Time
u,v,w	Shell displacements
WA	Dimensionless angular velocity
z, \bar{z}	Dimensionless shell deflection w/a .

Greek Letters

α^2	$h^2/12a^2$, a dimensionless constant
μ	Poisson's ratio
ρ	Material density in shell
Ω	Shell angular velocity
ϵ	Strain
$\bar{\Omega}$	Dimensionless shell angular velocity
τ	Dimensionless time
θ	Polar angle
θ_1	$\theta - \Omega t$, a moving co-ordinate

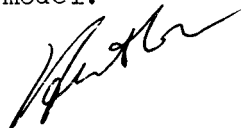
I. ABSTRACT

23669

An elastically supported cylindrical shell is used as a model for the dynamic rolling of a loaded pneumatic tire. Such a model includes many of the effects found in the real tire, such as bending of the tread in the contact patch region, elastic support coming from the inflated sidewalls and loss effects coming from the inherent dissipative properties of the materials used.

Methods are presented for calculating the dynamic contact patch areas of such a model, and it is shown that these are influenced considerably by rolling velocity, the constructional parameters of the tire and its loss characteristics. Dynamic pressure distributions inside these contact patch areas may also be obtained analytically, and techniques are given for doing this.

As an example of the use of such a model, an elastically supported cylindrical shell with a viscous loss law is used as a basis for the calculation of the load carrying and drag properties of a pneumatic tire, to the extent that the various tire parameters may be approximated. These results are presented as typical of the information which may be obtained from such a model.



II. INTRODUCTION

It is a reasonably good approximation to state that most pneumatic tire problems can be separated into two groups, these being:

- (a) Those involving motion in the plane of the wheel or rim;
- (b) Those involving motion transverse to the plane of the wheel or rim.

There are, of course, occasional exceptions to this compartmentalization, but in the main it is felt that considerable knowledge could be gained by developing methods for separately studying pneumatic tire performance either in the plane of the wheel or transverse to the plane of the wheel.

Preliminary efforts have been made by such writers as Saito¹ and Thorsen² in developing techniques for predicting cornering forces and other effects transverse to the plane of the wheel. To the best of the writer's knowledge, no systematic attempts have been made to study motion in the plane of the wheel prior to Ref. 3. In that report, the use of an elastically supported cylindrical shell was proposed as a means for studying the static loading of a pneumatic tire against an infinitely rigid, frictionless plane. The results obtained from that analysis seemed to agree fairly well with contact patch length measurements made on real pneumatic tires.

In view of the many current problems associated with pneumatic tire motion in the plane of the wheel, it was felt desirable to attempt to extend these analytical techniques to those dynamic cases which can be profitably studied.

III. THE BASIC DYNAMIC MODEL FOR A ROLLING TIRE

We consider first a generalized cylindrical shell under arbitrary loads. This is shown in Figure 1, taken from Flugge.⁴

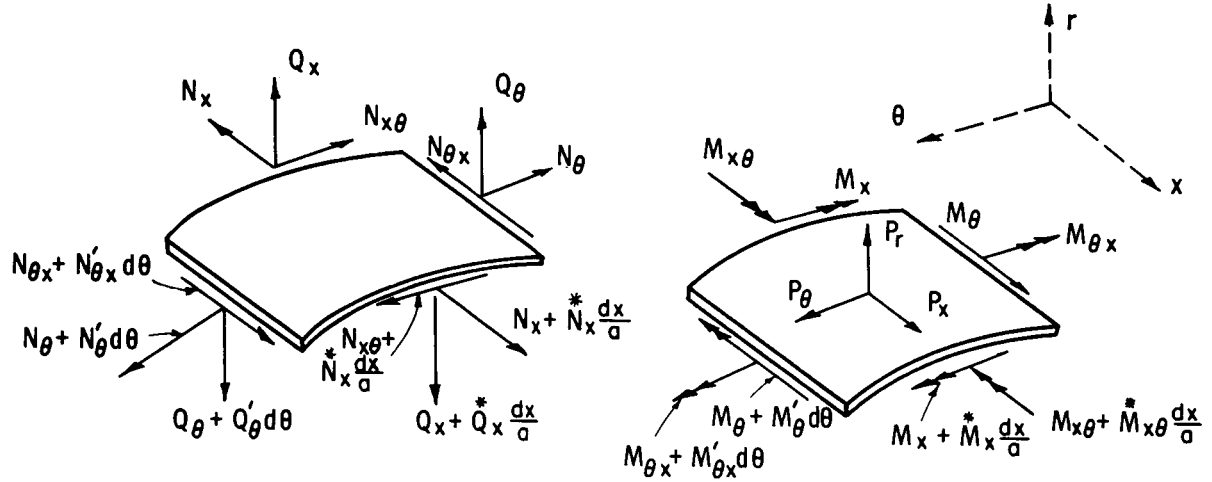


Figure 1. Shell stress resultant conventions and nomenclature.

From Figure 1, force equilibrium equations may be written for the element of cylindrical shell surface. Generally, these equations are directed in the x , θ , and r directions, and are given as:

$$\begin{aligned} \dot{N}_x + N'_{\theta x} + P_x \cdot a &= 0 \\ a N'_\theta + a \dot{N}_{x\theta} - M'_\theta - \dot{M}_{x\theta} + P_\theta a^2 &= 0 \\ M''_\theta + \dot{M}'_{x\theta} + \dot{M}'_{\theta x} + \dot{M}^*_{x\theta} + a N_\theta - P_r a^2 &= 0 \end{aligned} \quad (1)$$

The following symbols are used:

$$a \frac{\partial ()}{\partial x} = ()' \quad \frac{\partial ()}{\partial \theta} = () \cdot \quad (2)$$

It is next necessary to consider displacements of a cylindrical shell,

where we let

u = displacement along the generator, positive in the direction of increasing x ;

v = displacement along a circle of radius a , positive in direction of increasing θ ;

w = radial displacement, positive outward.

Using this notation, and assuming that: (1) all points lying on one normal to the middle surface before deformation do the same after deformation; (2) that for all kinematic relations the distance z of a point from the middle surface may be considered as unaffected by the deformations of the shell; (3) that the stress σ_r may be considered negligible compared with the stresses σ_x and σ_θ .

By use of such assumptions, and by consideration of the definitions of shell forces, one may finally express the various shell forces and moments in terms of the deformation by means of the equations

$$\begin{aligned}
 N_\theta &= \frac{\bar{D}}{a} (v' + w + \mu u^*) + \frac{K}{a^3} (w + w'') \\
 N_x &= \frac{\bar{D}}{a} (u^* + \mu v' + \mu w) - \frac{K}{a^3} w^{**} \\
 N_{\theta x} &= \frac{\bar{D}}{a} \cdot \frac{1 - \mu}{2} (u' + v^*) + \frac{K}{a^3} \cdot \frac{1 - \mu}{2} (u' + w') \\
 N_{x\theta} &= \frac{\bar{D}}{a} \cdot \frac{1 - \mu}{2} (u' + v^*) + \frac{K}{a^3} \cdot \frac{1 - \mu}{2} (v^* - w') \\
 M_\theta &= \frac{K}{a^2} (w + w'' + \mu w^{**}) \\
 M_x &= \frac{K}{a^2} (w^{**} + \mu w'' - u^* - \mu v') \\
 M_{\theta x} &= \frac{K}{a^2} (1 - \mu) (w' + \frac{u'}{2} - \frac{v^*}{2}) \\
 M_{x\theta} &= \frac{K}{a^2} (1 - \mu) (w' - v^*)
 \end{aligned} \tag{3}$$

If one uses Eqs. (3) and substitutes them into Eqs. (1), it is possible to obtain the three equations of equilibrium in terms of the three differential equations in displacements u , v and w of the middle surface of the shell. These equations become

$$\begin{aligned}
 & \ddot{u} + \frac{1-\mu}{2} u'' + \frac{1+\mu}{2} \dot{v}' + \mu \dot{w} + \alpha^2 \left[\frac{1-\mu}{2} u'' - \ddot{w} + \frac{1-\mu}{2} \dot{w}'' \right] + \frac{p x a^2}{\bar{D}} = 0 \\
 & \left(\frac{1+\mu}{2} \right) \dot{u}' + v'' + \frac{1-\mu}{2} \ddot{v} + w' + \alpha^2 \left[\frac{3}{2} (1-\mu) \ddot{v} - \frac{3-\mu}{2} \dot{w}' \right] + \frac{p \theta a^2}{\bar{D}} = 0 \\
 & \mu \dot{u} + v' + w + \alpha^2 \left[\frac{1-\mu}{2} \dot{u}'' - \ddot{u} - \frac{3-\mu}{2} \ddot{v}' + \ddot{w} + 2 \dot{w}'' + w'''' \right. \\
 & \quad \left. + 2 w'' + w \right] - \frac{p r a^2}{\bar{D}} = 0
 \end{aligned}
 \tag{4}$$

We next wish to consider the specific case of a rather narrow cylindrical shell which has no variation of loading with respect to the x direction. In this case, the shell takes on the form shown in Figure 2, where a shell of width b_w and thickness h is made of material of modulus E and density ρ , the radius of the cylinder being a .

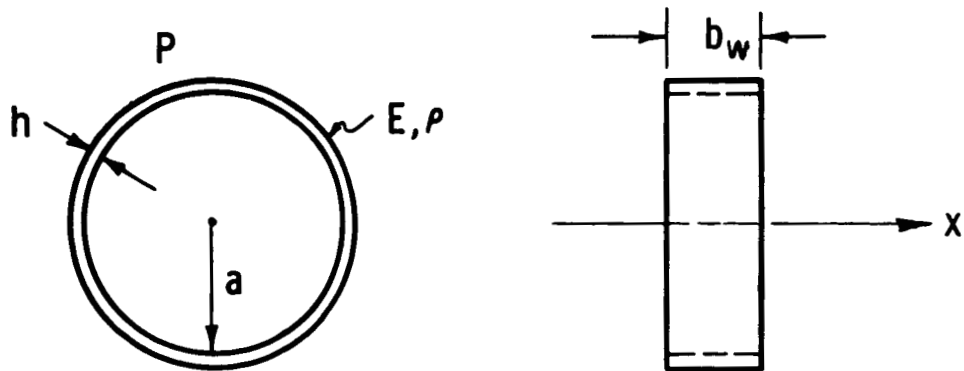


Figure 2. Narrow cylindrical shell notation.

If the loading is uniform with respect to the x direction, and if the width b_w is small enough so that contraction in the x direction may be neglected, then one may visualize that all derivatives with respect to x in Eqs. (4) will vanish. In addition, all displacements u in the x direction become negligible and will be dropped, as will pressure components in the x direction. Allowing these simplifying assumptions to be used in Eqs. (4) causes them to reduce to

$$\begin{aligned} \frac{\partial}{\partial \theta} \left(\frac{\partial v}{\partial \theta} + w \right) + p_\theta \frac{a^2}{D} &= 0 \\ \left(\frac{\partial v}{\partial \theta} + w \right) + \alpha^2 \left[\frac{\partial^4 w}{\partial \theta^4} + 2 \frac{\partial^2 w}{\partial \theta^2} + w \right] - \frac{Pr^a}{D} &= 0 \end{aligned} \quad (5)$$

There are several ways that one may proceed to analyze Eqs. (5). Perhaps the simplest of these is to visualize that for a frictionless plane p_θ vanishes so that the first of Eqs. (5) simply states that

$$\left(\frac{\partial v}{\partial \theta} + w \right) = \text{Cons't} \quad (6)$$

This same term occurs in the second of Eqs. (5). It is immediately recognized as being connected to the circumferential membrane strain through the well known relation

$$\epsilon_{\theta_m} = \frac{1}{a} \left(w + \frac{\partial v}{\partial \theta} \right) \quad (6a)$$

It is simplest to carry this term along in the equations for some time before assigning it a specific value. Hence, Eqs. (5) may now be written

$$a\epsilon_{\theta m} + \alpha^2(w^{IV} + 2w'' + w) = \frac{Pr a^2}{En} \quad (7)$$

This equation now represents the equation for deflection of a cylindrical shell against a frictionless load, so that only radial pressures exist. Note that the constant α^2 is given by

$$\alpha^2 = \frac{h^2}{12a^2}.$$

In Eq. (7), it is desirable to include most of the properties of a real pneumatic tire by means of adjusting the radial pressure term p_r for various tire effects. Specifically, it is desired to support the elastic shell by means of some kind of generalized impedance in such a way that both real elastic moduli and imaginary elastic moduli can be operative. This might be thought of, in some respects, as filling the inside of the shell with a massless foam-like material. For purposes of this report, the generalized impedance will be reduced to the specific case of a real elastic and viscous loss support system, but it is readily understood that the viscous loss support mechanism may be replaced by other mechanisms such as a hysteresis type of loss. For the present, the viscous loss mechanism represents a very simple device which is easily treated analytically, and for that reason will be retained here.

As an additional feature of Eq. (7), it is desirable to include both a uniform internal inflation pressure and an external pressure loading term denoting contact pressures coming from contact with the ground surface.

Finally, inertia terms form part of the radial loading since it may be anticipated that the shell in question will be accelerating in the w direction as well as being subjected to an overall rigid body rotation of angular velocity Ω . Accounting for all of these factors, one may write the total radial pressure of the shell in the form

$$\begin{aligned}
 (a) \quad p_r &= -\rho h [\ddot{w} - (a + w)\Omega^2] & (c) \quad p_r &= cw \\
 (b) \quad p_r &= -kw & (d) \quad p_r &= p_o \\
 (e) \quad p_r &= -p(\theta) & & (8)
 \end{aligned}$$

assuming that tangential velocities are negligible and where

$$\frac{\partial(\quad)}{\partial t} = (\dot{\quad})$$

Including all of these effects into Eq. (7), one finally obtains

$$\begin{aligned}
 a\epsilon_{\theta_m} + \frac{a^2 w}{c_1^2} + \frac{a^2 c}{Eh} \dot{w} + \alpha^2 w^{IV} + 2\alpha^2 w'' \\
 + w[\alpha^2 + \frac{ka^2}{Eh} - \frac{\Omega^2 a^2}{c_1^2}] = \frac{a^2}{Eh} [p_o - p(\theta) + \rho h a \Omega^2]
 \end{aligned} \tag{9}$$

In this equation, the presence of the Ω^2 term is due to the fact that the shell is assumed to be rotating with angular velocity Ω . We will next allow loads to move in the opposite direction to Ω around the periphery of the rotating shell by means of transforming the shell equations into a new independent variable

$$\begin{aligned}
 \theta_1 &= \theta - \Omega t \\
 \frac{\partial(\quad)}{\partial t} &= \frac{\partial(\quad)}{\partial t} - \Omega \frac{\partial(\quad)}{\partial \theta_1} \\
 \frac{\partial^2(\quad)}{\partial t^2} &= (\ddot{\quad}) - 2\Omega(\dot{\quad}) + \Omega^2(\quad)''
 \end{aligned} \tag{10}$$

Using these, one obtains

$$\begin{aligned}
 a\epsilon_{\theta_m} + \frac{a^2}{c_1^2} (\Omega^2 w'' - 2\Omega \dot{w}' + \dot{w}) + \frac{a^2 c}{Eh} (\dot{w} - \Omega w') \\
 + \alpha^2 w^{IV} + 2\alpha^2 w'' + w \left[\alpha^2 + \frac{ka^2}{Eh} - \frac{\Omega^2 a^2}{c_1^2} \right] \\
 = \frac{a^2}{Eh} [-p(\theta) + p_0 + \rho h a \Omega^2]
 \end{aligned} \tag{11}$$

where

$$c_1^2 = E/\rho .$$

Next, introduce the new variables (see Ref. 5)

$$\frac{w}{a} = z ; \quad \frac{tc_1}{a} = \tau ; \quad c_1^2 = \frac{E}{\rho} \tag{12}$$

from which the equation of motion of the shell may now be written in the form

$$\begin{aligned}
 \epsilon_{\theta_m} + \ddot{z} + \frac{acc_1}{Eh} \dot{z} - \frac{2a\Omega}{c_1} \dot{z}' + \alpha^2 z^{IV} \\
 + (2\alpha^2 + \frac{a^2 \Omega^2}{c_1^2}) z'' - \frac{a^2 c \Omega}{Eh} z' \\
 + (\alpha^2 + \frac{ka^2}{Eh} - \frac{\Omega^2 a^2}{Eh}) z = \frac{a}{Eh} [-p(\theta) + p_0 + \rho h a \Omega^2]
 \end{aligned} \tag{13}$$

Introducing the variable

$$\frac{\Omega a}{c_1} = \bar{\Omega} \tag{14}$$

one finally obtains Eq. (13) in the form

$$\begin{aligned}
 \epsilon_{\theta_m} + \ddot{z} + \frac{acc_1}{Eh} \dot{z} - 2\bar{\Omega} \dot{z}' + \alpha^2 z^{IV} + (2\alpha^2 + \bar{\Omega}^2) z'' \\
 - \frac{acc_1}{Eh} \bar{\Omega} z' + (\alpha^2 + \frac{ka^2}{Eh} - \bar{\Omega}^2) z \\
 = \frac{a}{Eh} [-p(\theta) + p_0 + \rho h a \Omega^2] .
 \end{aligned} \tag{15}$$

In Eq. (15), we define the new constants as follows:

$$\begin{aligned}\frac{ac_1c}{Eh} &= \bar{c} & \frac{a n(\theta)}{Eh} &= PE \\ \frac{ap_0}{Eh} &= PO\end{aligned}\tag{16}$$

and dividing by α^2 , one finally obtains the equation of motion

$$\begin{aligned}\frac{\epsilon_{\theta m}}{\alpha^2} + \frac{\ddot{z}}{\alpha^2} + \frac{\bar{c}}{\alpha^2} \dot{z} - \frac{2\bar{\Omega}^2}{\alpha^2} \dot{z}' + z^{IV} + (2. + \frac{\bar{\Omega}^2}{\alpha^2})z'' - \frac{\bar{c}}{\alpha^2} \bar{\Omega} z' \\ + (1. + \frac{\bar{k}}{\alpha^2} - \frac{\bar{\Omega}^2}{\alpha^2})z = - \frac{PE}{\alpha^2} + \frac{\bar{\Omega}^2}{\alpha^2} + \frac{PO}{\alpha^2}\end{aligned}\tag{17}$$

where

$$\bar{k} = \frac{ka^2}{Eh}.$$

Equation (17) is an equation for motion of the cylindrical shell and contains all terms necessary for representing most of the phenomena which can be observed in a rolling pneumatic tire. Loss terms are represented through the viscous loss constant \bar{c} , dynamic terms through the quantity $\bar{\Omega}$ and elastic terms through the quantity \bar{k} . The angular velocity of the wheel is given by the dimensionless angular velocity $\bar{\Omega}$ so that Eq. (17) in effect represents a circular cylindrical shell, supported as indicated in Figure 3, with a moving load of angular velocity Ω . In addition to this angular velocity Ω , one may superimpose a rigid body rotation of angular velocity Ω in the opposite direction, as was done with the inertia term of the form $(a + w)\Omega^2$ in Eq. (8). This term, whose effect is to superimpose the rigid body rotation of angular velocity Ω on the entire system, results in Eq. (17) now representing rotating tire with stationary impressed load, such as is shown in Figure 3.

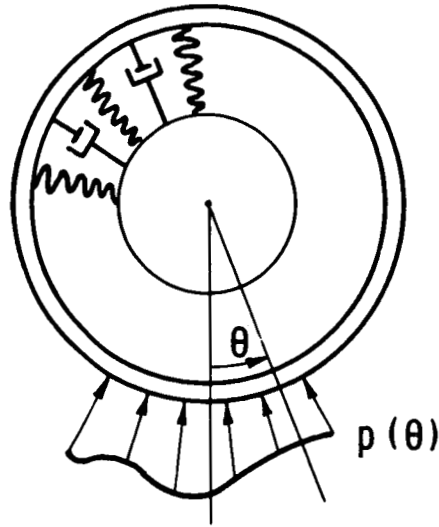


Figure 3. Shell characteristics.

We now consider steady state solutions to Eq. (17). Under this condition, all time derivatives vanish and making substitutions of constants in the form

$$\frac{\bar{\Omega}^2}{\alpha^2} = WA; \quad \frac{\bar{c} \bar{\Omega}}{\alpha^2} = CWA; \quad \frac{\bar{k}}{\alpha^2} = KA \quad (18)$$

$$\frac{PE}{\alpha^2} = P\theta \quad \frac{PO}{\alpha^2} = PA$$

one sees that this reduces to

$$\begin{aligned} \frac{\epsilon_{\theta m}}{\alpha^2} + z^{IV} + (2 + WA)z'' - (CWA)z' + (1 + KA - WA)z \\ = PA - P\theta + WA \end{aligned} \quad (19)$$

where, of course, the primes represent derivatives with respect to the variable θ_1 , and in general Eq. (19) represents steady state, or standing wave, solutions to the deformation of the rotating cylindrical shell.

It is now necessary to define the constant $\epsilon_{\theta m}/\alpha^2$. This will be done by making the following basic assumptions:

- (a) The process of inflation will be considered as one involving membrane effects only.
- (b) The process of deforming the tire in the contact patch will be considered as one involving bending effects only.

Based on these ideas, we may let

$$\frac{\epsilon_{\theta m}}{\alpha^2} = \frac{1}{\alpha^2} \left[\frac{p_o^a}{Eh} \right] \quad (20)$$

which implicitly defines the dimensionless displacement z as being measured from the inflated position. Using this, Eq. (19) may be written in the form

$$\bar{z}^{IV} + (2 + WA)\bar{z}'' - (CWA)\bar{z}' + (1 + KA - WA)\bar{z} - WA = - P\theta \quad (21)$$

where \bar{z} is used to emphasize that this displacement is measured from the inflated tire as a reference. From this equation, one sees that the static problem may be obtained readily by allowing the values of WA and CWA both to vanish simultaneously. This causes Eq. (21) to reduce immediately to

$$\bar{z}^{IV} + 2\bar{z}'' + (1 + KA)\bar{z} = - P\theta \quad (22)$$

which was used in Ref. 3.

IV. THE CONTACT PATCH REGION

There are two problems associated with attempting to define the region or length of contact of the tire model pressed against a frictionless plane. The first of these is the determination in some form or another of some of the elastic constants which fit into the various equations of motion just developed, particularly Eq. (21), which is the primary statement of deformation from the inflated state.

One method of accomplishing this is to observe that the static case of Eq. (21), given in this report as Eq. (22), indicates that the static problem of contact is a relatively simple one involving only a single elastic constant, the dimensionless foundation modulus denoted here by the symbol KA . It should be possible to determine the value of KA by appropriate tests on various real tires, in which certain deflections are imposed and the resulting contact patch lengths are measured. Experiments indicate that this may indeed be done.

Similar techniques have not yet been developed for the direct measurement of other elastic constants appearing in Eq. (21). For purposes of this report, tire construction may be used as a guide in calculating some of the constants appearing in this equation, and in this regard we are rather fortunate in having available a background in the material properties of cord rubber laminates. By the use of such information one could generally hope to obtain the remaining constants necessary in Eq. (21).

In connection with Eq. (21), one must next decide on techniques for treating the deformation of the cylindrical shell model against a frictionless plane.

In doing this, it is seen that the left side of the equation contains terms involving deflections while the right side contains only the external pressure loading term. If one could know the deflections of the shell model inside the contact patch region, then it might be possible to specify the values z on the left side of Eq. (21) and to calculate the particular values of θ for which the external pressure vanished, by means of the right side vanishing in Eq. (21). This may be accomplished by reference to Figure 4 from which one may deduce by geometry that

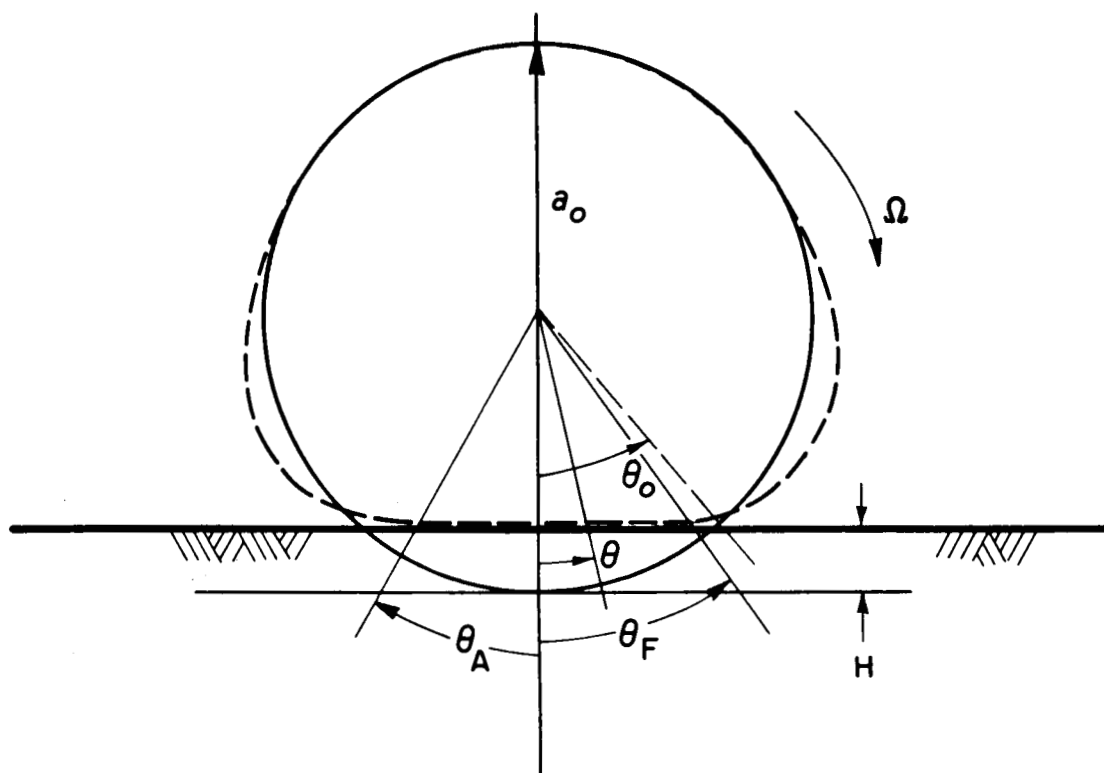


Figure 4. Geometry of intersection of elastic shell with a rigid plane surface.

$$\bar{z} = - \left(1 - \frac{\cos \theta_0}{\cos \theta} \right) \quad (23)$$

where

$$\bar{z} = \frac{w}{a_0} .$$

The first, second and fourth derivatives of this function are needed, and these work out to be

$$\bar{z}' = \frac{\cos\theta_0}{\cos\theta} \left(\frac{\sin\theta}{\cos\theta} \right) \quad (24)$$

$$\bar{z}'' = \frac{\cos\theta_0}{\cos\theta} \left(\frac{1 + \sin^2\theta}{\cos^2\theta} \right) \quad (25)$$

$$\bar{z}^{IV} = \frac{\cos\theta_0}{\cos\theta} \left[\frac{5 + 18 \sin^2\theta + \sin^4\theta}{\cos^4\theta} \right] \quad (26)$$

Having these derivatives, it may be seen at once that given the proper elastic constants all terms of Eq. (21) may be evaluated by using Eqs. (23) - (26), which physically mean that the outer surface of the shell is in contact with the flat plane of Figure 4. We then search for the pressures $P\theta$ in Eq. (21) which cause this situation to occur. Inside the region of the contact patch such pressures will be positive, while outside the contact patch region such pressures will be negative. Thus, we search for solutions to Eq. (21) in which the right hand side is zero. Such solutions must be functions of the angle θ , and such solutions thus give angles θ which define the ends of the contact patch.

Note that all functions on the left side of Eq. (21) are even except for the first derivative function which occurs in connection with the damping term. If the damping is nonzero, then it may be seen that the forward and aft angular locations of the contact patch will not be equal to one another, and in general this has been observed to be a fact. Use of Eq. (21) thus gives dynamic information concerning the contact patch in a rolling tire under the assumptions of complete contact with the flat plane.

In a later section of this paper a specific example of the calculation of contact patch length under dynamic conditions will be presented. For the moment, the theory is complete and need only be worked out for the proper numerical cases.

V. CALCULATIONS AND EXAMPLES

There are at least two methods for attempting to verify some of the theoretical ideas brought out by the use of a model such as proposed in this report. Perhaps the best and most direct of these would be to manufacture a model of the type visualized here and to actually conduct tests involving its rolling over some essentially frictionless plane, in such a way that pressure distributions, total vertical loads and drag forces could be measured accurately. If the properties of the model were well known, then the predictions of the theory could be compared with measured data. However, such a series of experiments becomes rather difficult when they must be done on a flat plane as visualized here, since the equipment for rolling a wheel on such a flat surface is expensive and complicated. For that reason a different approach will be used here, where one attempts to utilize physical data which closely approximates that of a real tire, and attempts to predict some of the known operating characteristics of such a tire. In some respects this is less satisfactory than the first process, since it is known that many of the important operating characteristics of a tire depend heavily on the form of its internal loss. These internal loss characteristics are not necessarily well defined for rubber-cord combinations. It is clear that a simple viscous loss law does not represent such loss characteristics very well, but its form is quite simple and will serve to illustrate the method of calculation. For this reason it should be pointed out clearly that the purpose of this example is not to model a specific tire exactly, but rather to introduce a technique which, given the

proper loss characteristics, can be used to perform such modeling. Hence, the resulting calculations are only indications of the general nature of tire behavior under such conditions. The fact that some of the important characteristics seem to agree with actual tire characteristics gives hope that the theoretical framework outlined here will have some utility as a tool in predicting the response of a real pneumatic tire.

One must first turn to the constants needed in evaluating Eq. (21). Basically, these constants are exactly those which one must use to define the overall characteristics of a circular cylindrical shell of the type proposed here. An attempt has been made to choose such characteristics to be compatible with a 7.50 x 14.00 automotive tire, and the resulting numerical values are being used for subsequent calculations.

$$\begin{aligned}
 b_w &= 4.25 \text{ in.} & E &= 10,000. \text{ psi} \\
 a &= 12.35 \text{ in.} & h &= 1.14 \text{ in.} \\
 a_o &= 13.35 \text{ in.} & \rho &= 1 \times 10^{-4} \text{ lb-sec}^2/\text{in.}^4
 \end{aligned}
 \tag{27}$$

Using this particular value of the outside radius of the wheel a_o , namely 13.35 in., one finds that the angular velocity is related to the linear speed in miles per hour by the relation

$$\Omega = 1.32 \text{ rad/sec/mph.}
 \tag{28}$$

Consider next the problem of calculating the response of a pneumatic tire having the properties given in Eqs. (27) under conditions of given velocity and load. For this purpose, one must first specify the loss law to be used. The viscous loss type of law previously discussed will be utilized here, and the damping factor c will be chosen as

$$c = 0.10 \quad (29)$$

This is based on interpretation of oscillograph records from free vibration tests of a pneumatic subjected to an impulsive blow.

A digital computer program has been constructed which first calculates the forward and aft edges of the contact patch at a fixed value of damping constant, and for various values of the other parameters listed in Eqs. (27) and (28). This is done by specifying the tire deflection, which is effectively accomplished by fixing the angle Θ_0 of Eq. (23) or of Figure 4. Once the limits of the contact patch are known, one may utilize Eqs. (21) and (23) - (26) to calculate the pressure distribution in the contact patch. Given the pressure distribution, the total load and the drag force may be obtained by integration. For this example, the vertical tire deflection will be allowed to vary from 0.5 to 2.0 inches. The linear velocity will be allowed to range from 0 to 120 miles per hour and the inflation pressure will take on four values, 0, 15, 24 and 40 psi.

In these calculations, it is necessary to have some value for the dimensionless foundation modulus $\bar{k}/\alpha^2 = KA$. It was previously pointed out that this quantity can be obtained directly from a static test in which the length of the length of the contact patch is measured, and for the particular tire in question a value of $KA = 325$ was obtained.

The results of these calculations are first given in Figure 5. Here, the forward and aft boundaries of a typical contact patch are plotted as a function of rolling velocity.

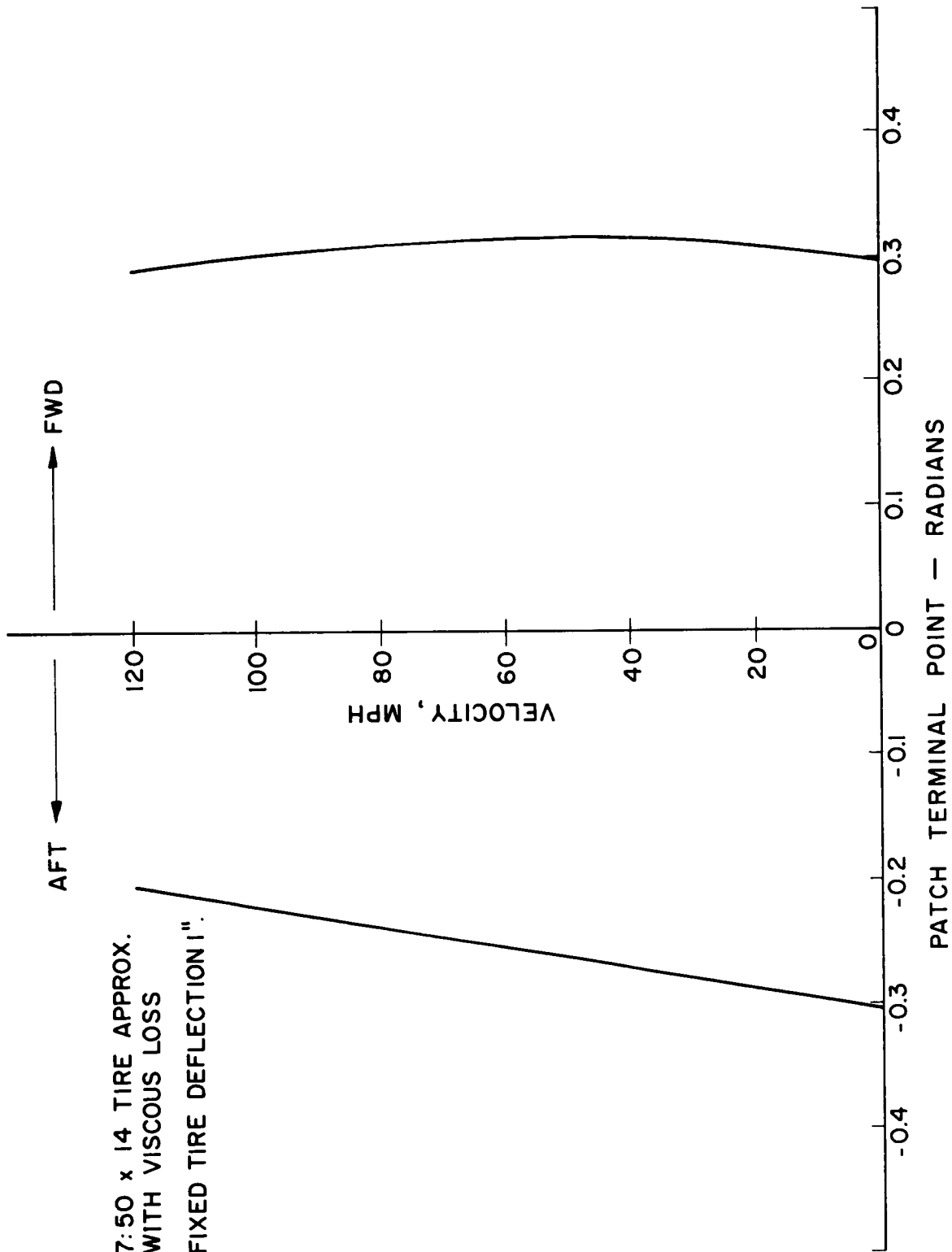


Figure 5. Contact patch length and position as a function of speed.

One might note from Figure 5 that, generally speaking, the tire exhibits a forward shift of the contact patch with speed, in that the forward and aft edges both move forward with velocity. This causes the entire pressure distribution to move forward and results in a shift of the center of pressure forward of the axle point so as to cause a drag force. This again seems to generally agree with experience.

In Figure 6 are shown curves of the influence of rolling velocity on vertical load carried at constant tire deflection. These curves are plotted for two different values of inflation pressures. Generally, the influence of speed is to increase load at fixed deflection. Conversely, at fixed load one would expect deflection to decrease with speed. Hence, rolling radius would increase with speed as has been observed.

In Figure 7, the drag force is plotted as a function of tire deflection for four different values of internal pressure, all data being calculated at a constant forward speed of 40 mph. These curves are almost entirely dependent upon the detailed form of the loss law which is assumed for this particular model, a viscous law with losses assigned only to the foundation. Nevertheless, the calculations do illustrate the general form of the results which are obtained, and show that even for this crude loss mechanism the drag force increases both with deflection and with inflation pressure, as it should. One advantage to plotting data in this fashion is that such constant speed plots eliminate some, but not all of the difficulties of the problem of correcting the loss law for temperature increases, and hence loss increases, as speed is increased. By restricting attention to a constant speed one does not

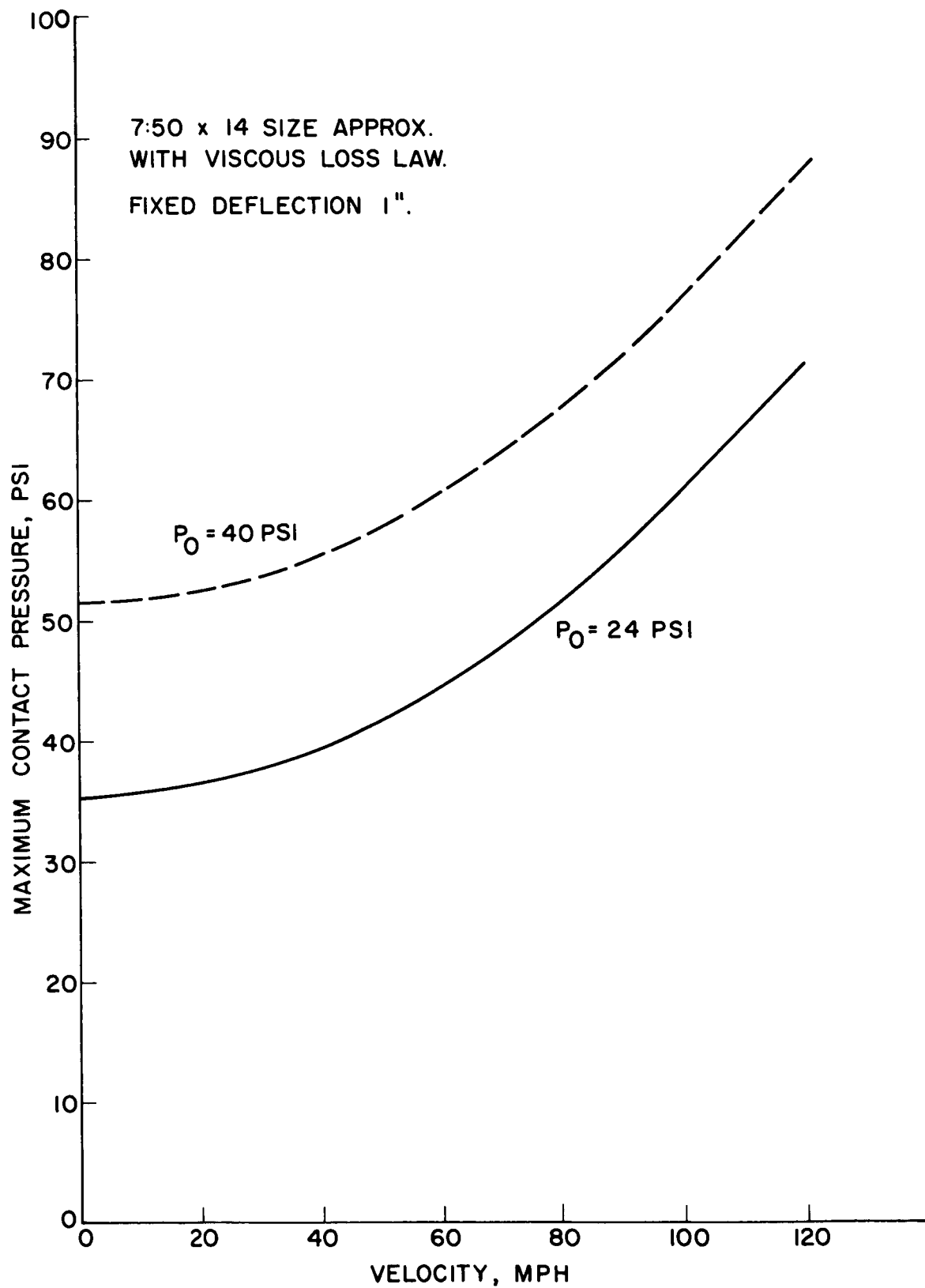


Figure 6. Vertical load as a function of speed.

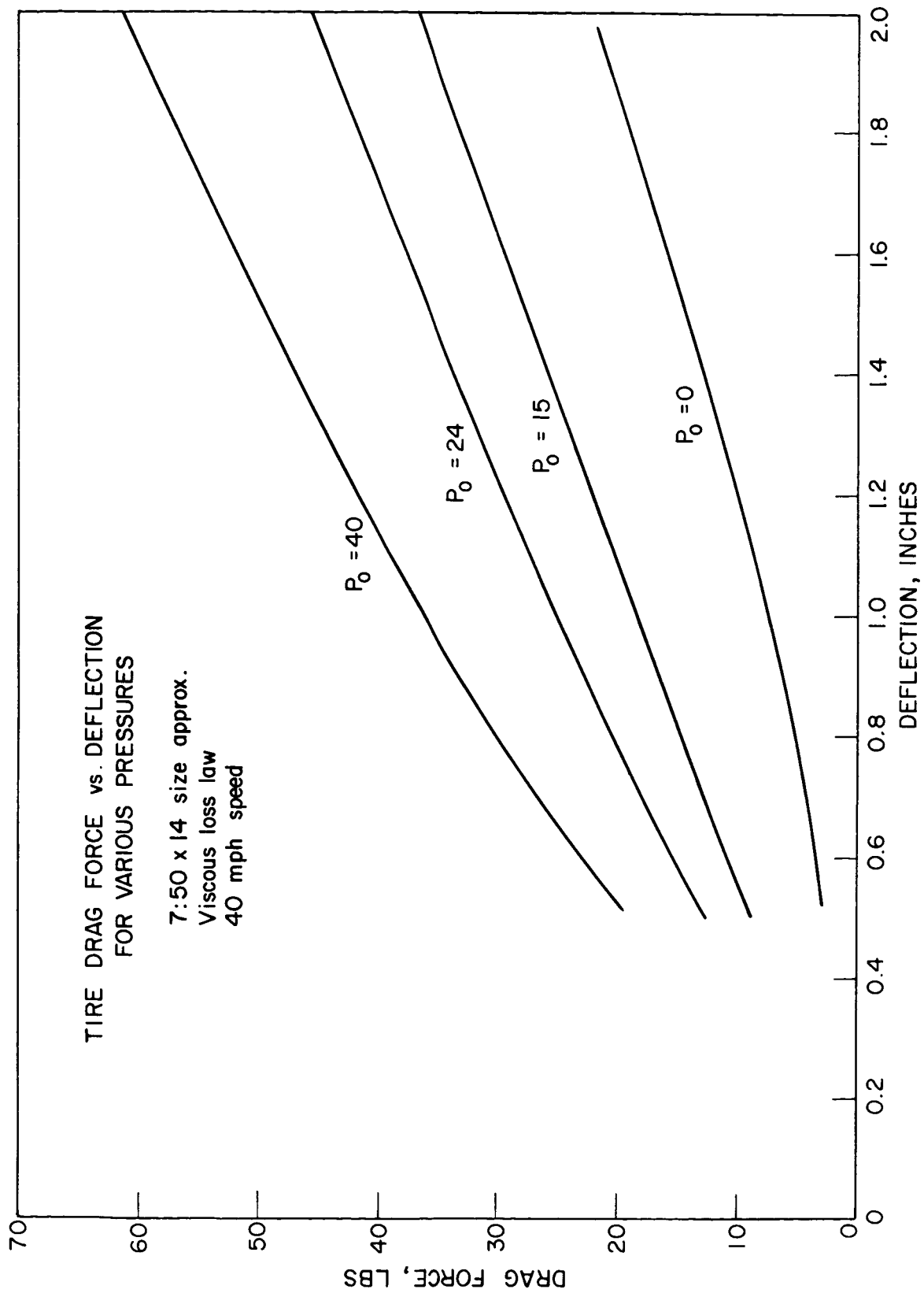


Fig. 7. Drag force as a function of speed.

see these temperature effects quite so clearly. It should also be noted that Figure 7 does not contain any loss from scrubbing in the contact patch, although this may be a small factor in the over-all picture. Figure 7 is intended as a general presentation of the type of information which can be obtained by calculation from this model, and should not be interpreted as representing the characteristics of the general model.

In Figure 8, the maximum contact pressures in the contact patch are plotted as a function of rolling velocity for the same two internal pressures as previously treated. The results shown in Figure 8 seem to indicate that at the usual inflation of 24 psi, contact pressures would normally not exceed 40 psi under ordinary driving conditions.

Figure 9 shows plots of the contact pressure distribution in the contact patch at two different speeds, 0 and 100 miles per hour for a single inflation pressure. The static pressure distribution is symmetric and almost rectangular. On the other hand, the dynamic pressure distribution evaluated at 100 miles per hour shows rather large differences between the peak pressure near the center of the contact patch and the inflation pressure. In addition, the entire pressure distribution has shifted forward. This causes a forward movement of the center of pressure which results in drag forces.

So far all of the results presented have been speculative in the sense that good experimental data have not been available as a check. However, there is one static quantity which can be easily measured, and that is the load deflection curve. The particular tire which was being modeled here was inflated to various pressures and loaded to obtain such curves. These results

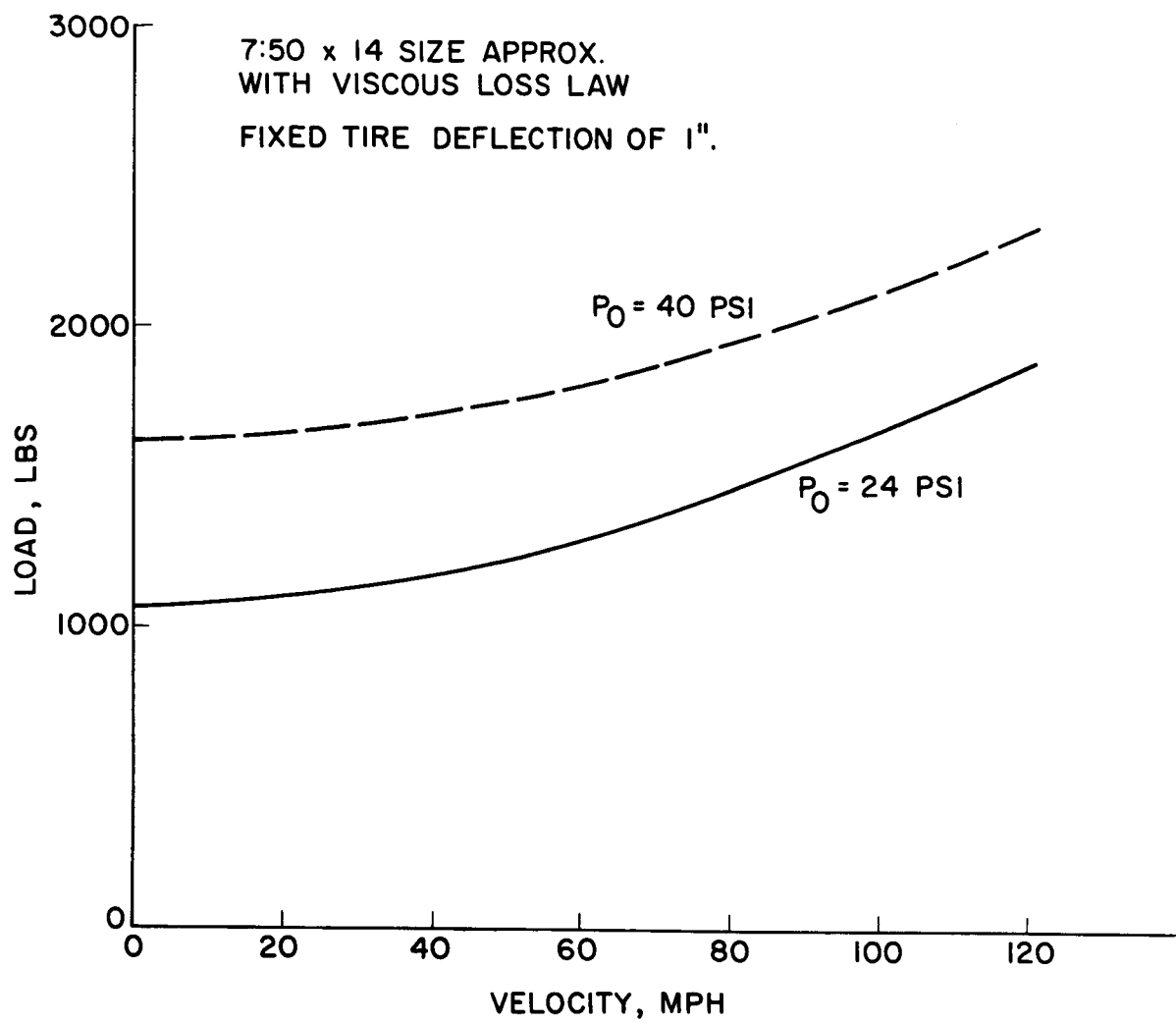


Figure 8. Maximum contact pressure as a function of speed.

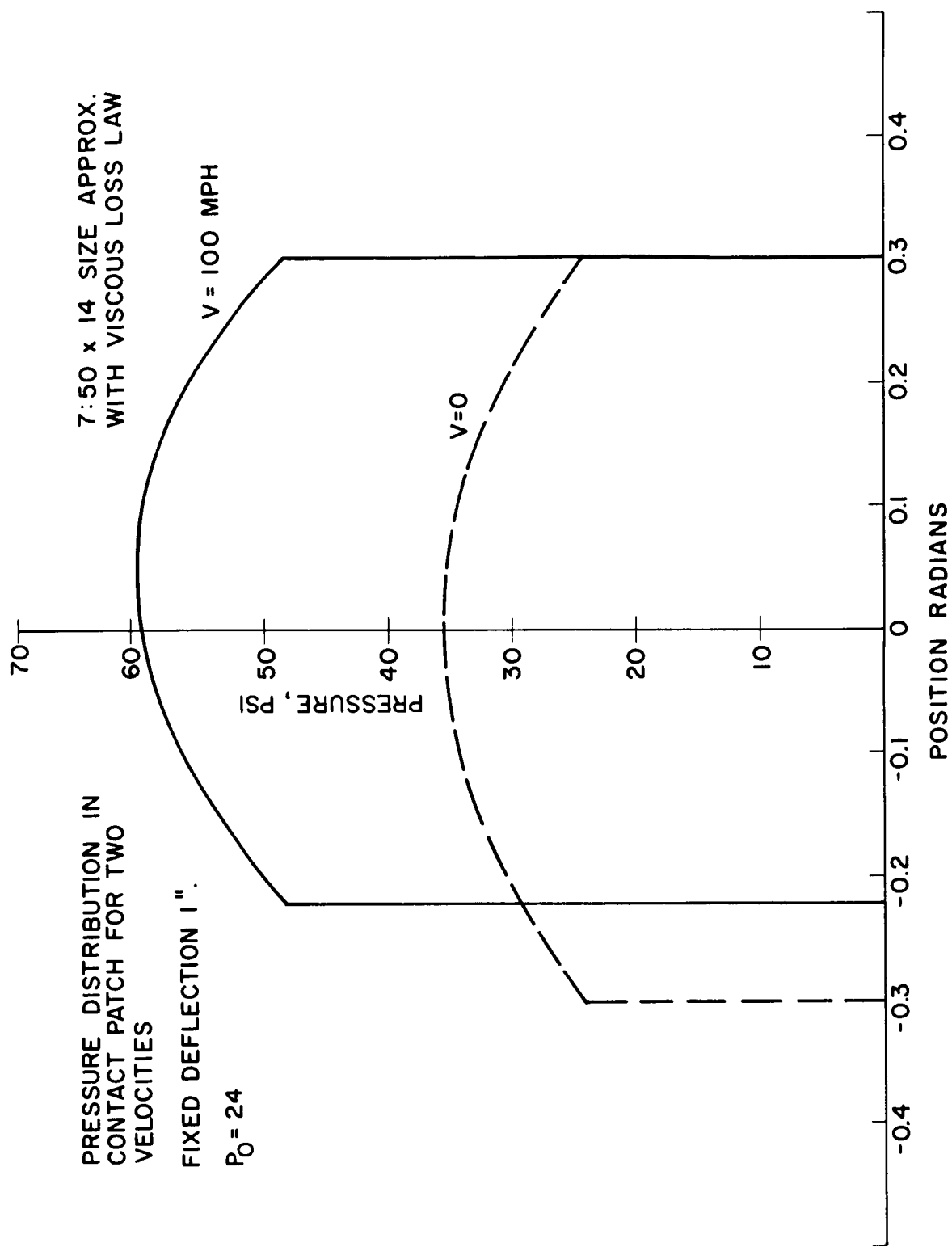


Figure 9. Pressure distribution in contact patch for two different velocities.

are compared with calculation in Figure 10, where it is seen that predictions tend to be a little more accurate at lower deflections than at higher, which might be expected from such a linearized theory.

In general it might be said that by use of the equations discussed in this paper it is possible to calculate many of the important quantities dealing with the rolling of a pneumatic tire in a straight line under constant velocity conditions. One very important characteristic in such calculations is the form of the loss law, since this determines almost completely the general form of the drag forces which are generated and also dictates to some extent the nature of the contact patch shift as velocity increases. Therefore, it should be emphasized that users of this type of mathematical model will probably find it necessary to generate their own individual loss laws and to insert them into the appropriate equations of this report. Only by this process will it be possible to obtain realistic tire performance data from a mathematical model such as this.

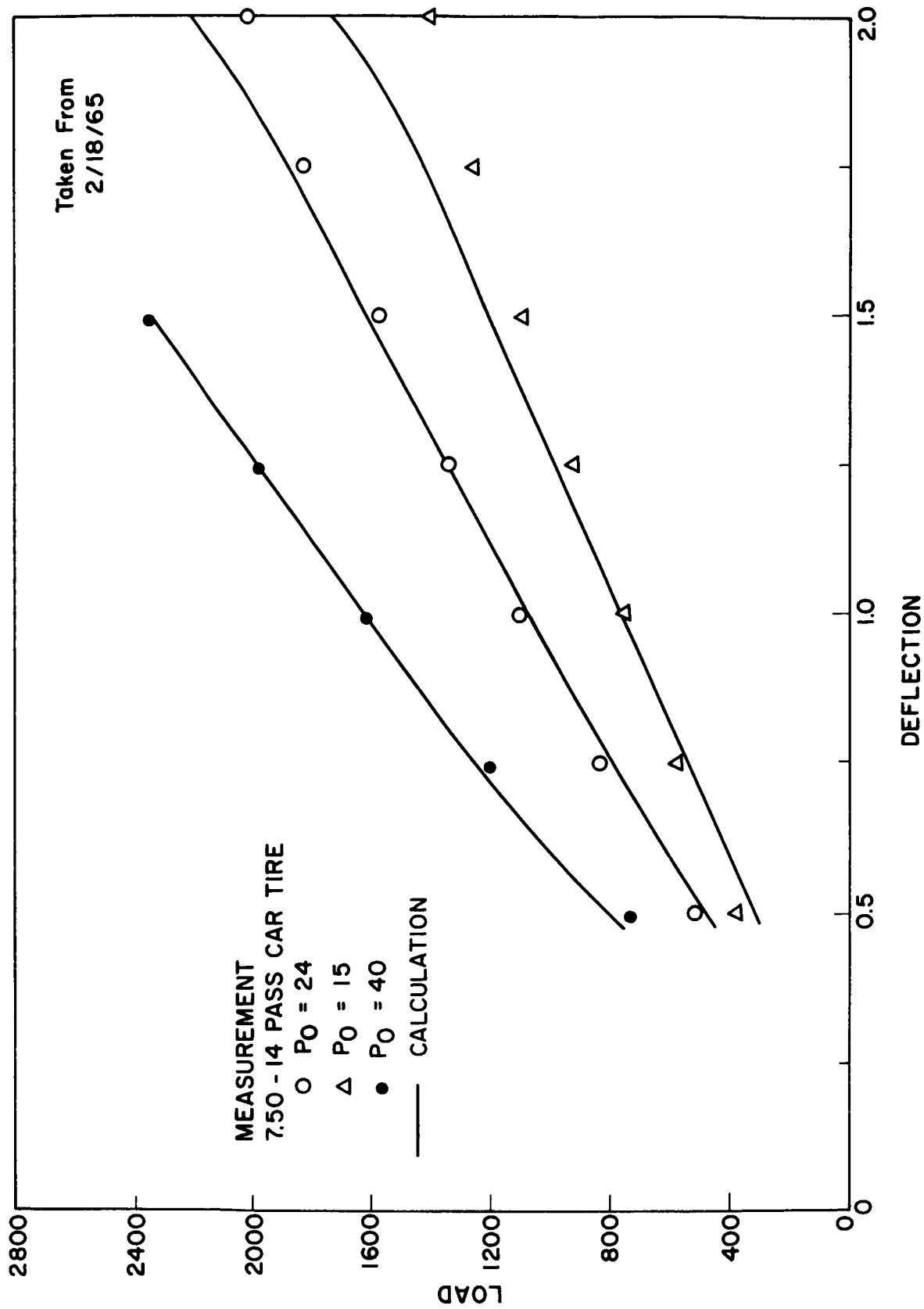


Figure 10. Static load deflection curves--experimental vs. calculated.

VI. REFERENCES

1. Saito, Y., "A Study of the Dynamic Steering Properties of Pneumatic Tires," 9th International Automobile Technical Congress, 1962, published by the Institution of Mechanical Engineers, London.
2. Thorsen, K. R., 1951 Boeing Airplane Company Report No. D-11719, "A Rational Method for Predicting Tire Cornering Forces and Lateral Stiffness."
3. Clark, S. K. "An Analog for the Static Loading of a Pneumatic Tire," The University of Michigan, Office of Research Administration, Report 02957-19-T. March 1964.
4. Flügge, Wilhelm, "Stresses in Shells," Springer-Verlag, Berlin, 1960.
5. Goodier, J. N. and McJvor, J. K., "The Elastic Cylindrical Shell Under Heavily Uniform Radial Impulse," A.S.M.E. Paper No. 63 APMW-6, 1963.